Available online at www.sciencedirect.com
ScienceDirect
International Journal of Mass Spectrometry 267 (2007) 248–255
www.elsevier.com/locate/ijms

A systematic study of ion and cluster ion formation in continuous supersonic planar plasma

H. Verbraak[a], D. Verdes[b], H. Linnartz[a,*]

[a] Sackler Laboratory for Astrophysics, Leiden Observatory, University of Leiden, Postbus 9513, NL 2300 RA Leiden, The Netherlands
[b] Institute for Physical Chemistry, University of Zürich, Winterthurerstrasse 190, CH 8057 Zürich, Switzerland

Received 2 November 2006; received in revised form 13 February 2007; accepted 21 February 2007
Available online 25 February 2007

Abstract

A systematic mass spectrometric survey has been performed to study ionic species that are formed in continuous supersonic planar plasma. The plasma is generated by electron impact ionization of gas that is expanded supersonically through a long and narrow slit. A quadrupole mass spectrometer is used to sample the adiabatically cooled plasma downstream for different precursor mixtures. The number of different ions and cluster ions formed in the plasma is remarkably large. Densities are sufficiently high to monitor rovibrational transitions in direct absorption by tunable diode laser spectroscopy, using concentration modulation and a phase sensitive detection scheme.

Keywords: Plasma expansion; Molecular ion; Ionic complex; Cluster ion; Quadrupole mass spectrometry

1. Introduction

In the last decade much progress has been made in generating dense plasma for high resolution spectroscopic studies of molecular transients, using supersonic expansions through long and narrow slits. Such two-dimensional plasma combines an effective adiabatic cooling with a nearly Doppler-free environment. In addition, absorption path lengths are relatively large and molecular densities are high. In combination with sensitive spectroscopic techniques, planar plasma expansions allow high resolution spectroscopic studies of a large variety of unstable species, complementing thermochemical data as available from the impressive work of late Lias [1–3]. Different types of planar plasma sources are operational nowadays and based upon discharge [4–6], photolysis [7], ablation [8] and electron impact ionization techniques [9]. Reported applications vary from small radicals [10], large and complex transients [11,12] to rovibrationally and rovibronically highly exited species [13,14]. One particular successful application in recent years has been the use of plasma expansions for direct absorption studies of ionic complexes and small cluster ions. The spectroscopy of an ionic complex – essentially the charged equivalent of a van der Waals complex – provides direct information on the fundamental properties of charged induced interactions [15–17]. These interactions (mainly charge transfer and proton bounding) are substantially stronger than pure van der Waals interactions and consequently binding energies are much higher. The charge transfer complex $[Ar–N_2]^+$ [18–20], for example, has a binding energy of nearly 1.2 eV and other species, such as the proton-sandwich $N_2–H^+–N_2$ [21] are readily produced in N_2/H_2 plasma. Chemical reactions in interstellar space and in the upper atmosphere are largely dominated by ion–molecule reactions [22]. Cluster ions have been proposed as transition states in proton transfer or charge exchange reactions and indeed protonated water dimer $[(H_2O)_2H]^+$ has been observed mass spectrometrically in the upper Earth's atmosphere [23]. Just very recently ionic complexes such as the $H_2–HCO^+$ and $[(CO)_2H]^+$ have been proposed as species of potential interstellar interest [24].

Systematic spectroscopic studies of ionic complexes have been limited for a long time because of experimental limitations. Vibrational predissociation spectroscopy has been applied very successfully to a large number of the more weakly bound cluster ions, both cations and anions [16,25]. Direct absorption studies as needed to study the more strongly bound species have been hindered by the lack of a source capable of producing

---

[*] Corresponding author. Tel.: +31 71 5275804; fax: +31 71 5275819.
E-mail address: linnartz@strw.leidenuniv.nl (H. Linnartz).

1387-3806/$ – see front matter © 2007 Elsevier B.V. All rights reserved.
doi:10.1016/j.ijms.2007.02.042

cluster ions in large abundances. The present study describes such a source as well as a systematic mass spectrometric survey to demonstrate its full potential. This also includes organic precursor molecules. One specific spectroscopic experiment is discussed in more detail to demonstrate how the unstable nature of a charged complex can be used to increase the detection sensitivity in a concentration modulation scheme.

2. Experiment—source and mass spectrometry

Supersonic plasma is generated by electron impact ionization of a gas that is expanded under pressure (200–1000 mbar) through a long and narrow slit (32 mm × 50 μm) into a vacuum chamber (see Fig. 1). The electrons are emitted by a tungsten wire (0.2 mm diameter) that is heated by a current of 4 A which is sufficient to heat the wire to the thermo-emission plateau. The wire is mounted parallel to the slit in a slotted molybdenum tube that acts as a Wehnelt shield condensing the cloud of primary emitted electrons. The tube is slightly negatively biased with respect to the filament and constrains the emitted electrons to an exit aperture parallel to the filament. In the vicinity of the tube aperture a space charge is generated due to the electrostatic confinement. Hence, the molybdenum tube acts as a convergent cylindrical lens and focuses the cloud of electrons towards the gas expansion. The electron beam is accelerated by the negative voltage of −150 V towards the nearest grounded metallic plate (anode), which is placed a few mm in front of the Wehnelt cylinder. A significant fraction of the electrons with a quasi-monochromatic energy crosses the slit aperture of the grounded anode and subsequent impact with the expanding gas ignites plasma and radical and ionic species are formed. The jet assembly can be moved back and forth with respect to the electron gun system; typically the distance is kept as small as possible. Plasma processes comprise direct electron impact, charge transfer and Penning ionisation. The plasma current flow between the filament (cathode) and the anode is measured using a small resistor (8 Ω) and is of the order of 30–40 mA. A constant current is maintained during the course of the experiment as any gradual changes in the plasma that occur due to filament degeneracy can be continuously corrected. This is essential to guarantee constant production conditions, particularly as minute amounts of reactive gases like hydrogen, oxygen and CO are sufficient to strongly initiate chemical reactions at the filament surface decreasing its life time. Furthermore, the complete electron gun system-consisting of the filament, the Wehnelt tube and the grounded anode is mounted to a water cooled copper block that assures a constant temperature during the experiment.

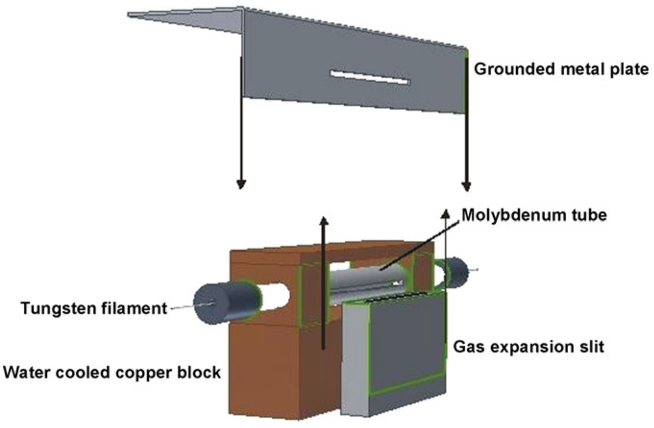

Fig. 1. A schematic 3D-drawing of the supersonic planar plasma source. See text for details.

A strong roots blower system (4800 m^3/h) is needed to keep the pressure below 0.1 mbar during plasma jet operation. In the expansion many processes take place simultaneously – hydrogen/proton attachment, proton transfer and charge exchange reactions, dissociative neutralization, and clustering – resulting in a quite unpredictable chemical mixture. Typical for a 2D expansion is the large number of collisions downstream in which besides ions also ionic complexes and cluster ions form. The latter survive the excess energy of the plasma as the adiabatic cooling results in low final temperatures. In order to characterize the plasma expansion and to optimize plasma conditions for a specific reaction product, a mass spectrometer has been incorporated in the setup. For this the central part of the expansion is dynamically skimmed by a 200 μm skimmer positioned 5 cm downstream. Ions that pass the skimmer enter a quadrupole mass spectrometer (QMS, model Balzers QMG 512) that is mounted in a second chamber, incorporated in the main chamber. Pressures are well below 10^{-6} mbar using differential pumping and (pump oil) pollutions are strongly reduced using a water baffle. The QMS is used to directly monitor charged plasma constituents, i.e., no additional filament ionization applies. Mass spectrometric signals are recorded using an oscilloscope that is read out by a computer. Generally cluster ion signals are visible by direct online monitoring, but also averaging is applied to visualize species that are harder to form.

A number of different gas mixtures has been used in order to systematically study the range of cluster ions that can be produced. Typical mixtures comprise different combinations of N_2, H_2 (D_2), CO_2, CO, H_2O and O_2, diluted and expanded in Ar, as well as a number of organic precursors.

3. Mass spectrometric results

In the case that hydrogen is present in the plasma proton transfer reactions dominate and mainly proton bound complexes are observed in the mass spectra. Such species consist of two or more atom/molecules bound by a proton; the charge is generally localized at the proton. A prototype example is the spectroscopically well studied $Ar–HN_2^+$ [26–32]. Without hydrogen, on the contrary, mainly charge induced complexes are observed (formed due to polarization, induction, and charge transfer), such as the important $[Ar–N_2]^+$ complex [18–20]. In this paragraph the formation of these two classes are addressed. In Figs. 2 and 3 typical mass spectra are shown for hydrogen plasma containing CO, N_2 and CO_2. Table 1a provides an overview of all ionic species formed in such plasma. Clear progressions $[(CO)_nH]^+$, $[(N_2)_nH]^+$, and $[(CO_2)_nH]^+$ are visible with maximum n-values (not shown in the figure) as high as 5, 7 and 7, respectively. The complexation efficiency depends on a combination of binding energy and backing pressure. The latter is varied only within a

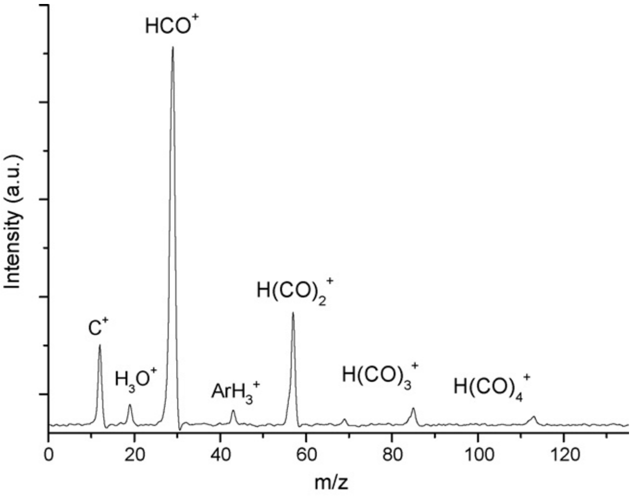

Fig. 2. A typical mass spectrum as recorded for expanding plasma with partial pressures of 400 mbar Ar, 30 mbar H_2 and 20 mbar CO.

small pressure regime as the source works in continuous modus and pump speed becomes critical rather easily. Using proton affinities as systematically catalogued by Lias and Huster [1] – 494.5 kJ/mol for N_2, 540.6 kJ/mol for CO_2 and 594 kJ/mol for CO – it is not clear why CO complexes seem to form less efficiently. A possible explanation may be related to a structural change; in the case of $[(N_2)_2H]^+$ a linear centro-symmetric (i.e., proton-sandwich) structure has been derived [21], whereas in the case of $[(CO)_2H]^+$ a linear but asymmetric OC–HCO^+ structure has been proposed [33]. This makes the OC–H^+-bond in $[OC–HCO]^+$ weaker than the N_2–H^+-bond in $[N_2–H–N_2]^+$, a process that may be extendable for larger clusters.

Mixed complexes are also formed in which the proton most likely acts as an intermolecular bridge. In Fig. 3 the formation of $[CO_2HN_2]^+$ is shown next to $[(N_2)_2H]^+$ and $[(CO_2)_2H]^+$. When extending the mass spectrum to higher masses (not shown in the figure) even more exotic complexes are found, e.g., $[(CO_2)_2HN_2]^+$, $[(CO_2)_2H(N_2)_2]^+$ and $[CO_2H(N_2)_3]^+$. Larger proton bound complexes are produced in smaller amounts, as more and more 3-body collisions are necessary to form these complexes. Abundances, therefore, are most likely higher further downstream and will increase for larger backing pressures, but for values above ∼1000 mbar the plasma becomes less stable.

Within the class of proton bound complexes, the protonated water clusters $[(H_2O)_nH]^+$ form a very important group. There still exists much debate on the actual structure of these clusters and this is particularly true for the protonated water dimer; gas phase infrared spectra have been recorded recently, but vibrational interpretations are still ambiguous [34–36]. The clusters are easily produced by flowing argon through a metal flask filled with water, after which the saturated gas is expanded through the slit nozzle. The mass spectrum in Fig. 4 shows a clear $[(H_2O)_nH]^+$ series starting at H_3O^+ and ending around $[(H_2O)_{14}H]^+$. For higher backing pressures larger clusters are formed. In a high pressure experiment, using a pulsed high pressure plasma expansion and time-of-flight analysis, n-values as high as 56 have been found [37] with stronger peaks at $n = 21$ and 28 that correspond to magic cluster sizes [38]. Adding small impurities into the gas mixture immediately results in the formation of species such as $[N_2–H_3O^+]$, $[CO–H_3O^+]$, and $[CO_2–H_3O^+]$.

When no hydrogen is added to the plasma, mainly charge induced complexes are formed (Table 1b). In general, such bonds are weaker than the proton bound equivalents, unless the ionization energies (IE) of the bonding partners are (approximately) the same. In this particular case molecular orbitals will have a significant overlap yielding a bond with a nearly covalent character and binding energies of 1–1.2 eV are found for homonuclear cluster ions such as $[(CO)_2]^+$ and $[N_2–N_2]^+$ but also a mixed cluster ion such as $[Ar–N_2]^+$ (IE(Ar) = 15.76 eV and

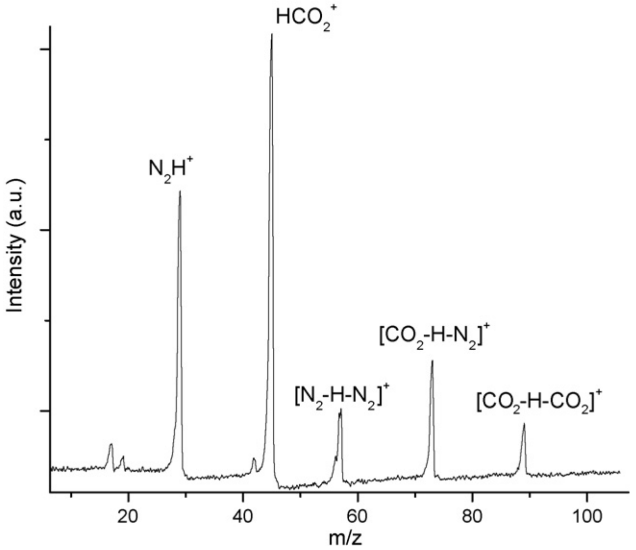

Fig. 3. A typical mass spectrum as recorded for expanding plasma with partial pressures of 400 mbar N_2, 20 mbar H_2 and 5 mbar CO_2.

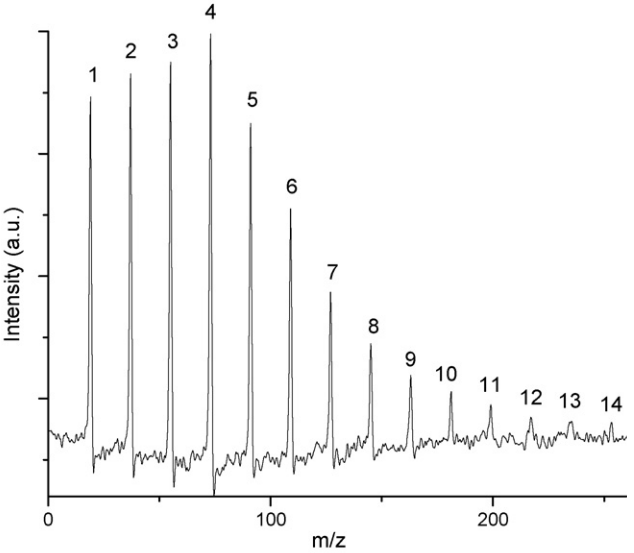

Fig. 4. A typical mass spectrum of expanding Ar/H_2O plasma. The cluster distribution depends on the backing pressure.

Table 1a
Overview of proton bound complexes formed in supersonic planar plasma using electron impact ionization

400 mbar N_2/ 60 mbar H_2														
m (amu)	17	19	29	42	45	57	85							
ion	NH_3^+	NH_5^+	N_2H^+	N_3^+	$N_3H_3^+$	$(N_2)_2H^+$	$(N_2)_3H^+$							
intensity	w	w	s	vw	vw	s	w							
500 mbar N_2/ 90 mbar H_2														
m (amu)	113	141	169	197										
ion	$(N_2)_4H^+$	$(N_2)_5H^+$	$(N_2)_6H^+$	$(N_2)_7H^+$										
intensity	w	w	vw	vw										
450 mbar Ar/ 20 mbar H_2/ 30 mbar CO_2														
m (amu)	45	73	89	117	133	161	177	221	265	309				
ion	CO_2H^+	CO_2HCO^+	$(CO_2)_2H^+$	$(CO_2)_2HCO^+$	$(CO_2)_3H^+$	$(CO_2)_3HCO^+$	$(CO_2)_4H^+$	$(CO_2)_5H^+$	$(CO_2)_6H^+$	$(CO_2)_7H^+$				
intensity	s	w	vs	w	a	vw	a	w	w	vw				
650 mbar Ar/ 20 mbar H_2/ ~5 mbar CO														
m (amu)	29	31	57	69										
ion	HCO^+	H_3CO^+	$(CO)_2H^+$	$ArHCO^+$										
intensity	vs	w	a	w										
350 mbar Ar/ 150 mbar H_2/ 300 mbar CO														
m (amu)	29	57	85	113	141									
ion	HCO^+	$(CO)_2H^+$	$(CO)_3H^+$	$(CO)_4H^+$	$(CO)_5H^+$									
intensity	vs	s	a	a	a									
300 mbar Ar/ ~5 mbar H_2/ ~5 mbar O_2														
m (amu)	32	33	35	41	65									
ion	O_2^+	HO_2^+	$H_3O_2^+$	ArH^+	$(O_2)_2H^+$									
intensity	s	s	vw	vw	w									
400 mbar N_2/ 20 mbar H_2/ ~5 mbar CO_2														
m (amu)	17	19	29	42	45	56	57	73	89					
ion	NH_3^+	NH_5^+	N_2H^+	N_3^+	CO_2H^+	N_4^+	$(N_2)_2H^+$	$N_2HCO_2^+$	$(CO_2)_2H^+$					
intensity	w	w	s	w	s	a	a	a	a					
Ar/ H_2/ CO/ CO_2														
m (amu)	57	69	73	89										
ion	$(CO)_2H^+$	$ArHCO^+$	$OCHCO_2^+$	$(CO_2)_2H^+$										
intensity	s	a	s	w										
Ar/ H_2/ N_2/ O_2														
m (amu)	32	33	35	57	61	65	69							
ion	O_2^+	HO_2^+	$H_3O_2^+$	$(N_2)_2H^+$	$N_2HO_2^+$	$(O_2)H^+$	$ArHN_2^+$							
intensity	s	w	s	s	s	s	a							
300 mbar Ar over H_2O														
m (amu)	19	37	55	73	91	109	127	145	163	181	199	217	235	253
ion	H_3O^+	$(H_2O)_2H^+$	$(H_2O)_3H^+$	$(H_2O)_4H^+$	$(H_2O)_5H^+$	$(H_2O)_6H^+$	$(H_2O)_7H^+$	$(H_2O)_8H^+$	$(H_2O)_9H^+$	$(H_2O)_{10}H^+$	$(H_2O)_{11}H^+$	$(H_2O)_{12}H^+$	$(H_2O)_{13}H^+$	$(H_2O)_{14}H^+$
intensity	vs	vs	vs	vs	s	a	a	a	w	w	vw	vw	vw	vw

The corresponding experimental conditions are listed. vs, very strong; s, strong; a, average; w, weak; vw, very weak.

$IE(N_2) = 15.58$ eV) has a binding energy of 1 eV. In this particular case there is a strong overlap between the $3p_z$ atomic orbital of Ar and the $3\sigma_g$ molecular orbital of N_2. A direct consequence is that in Ar/N_2 containing plasma not only species $[(N_2)_n]^+$ are efficiently formed – typically up to $[(N_2)_5]^+$ – but also $[Ar–(N_2)_n]^+$ ions are readily observed. This class of cluster ions, however, is in general less strongly bond. This is among others due to the fact that in proton bound complexes the charge is strongly localized on the proton whereas in charge induced complexes the charge is delocalized, and consequently, electrostatic interactions are weaker.

Fig. 5 shows a typical mass spectrum containing CO diluted with Ar. Clearly a progression $[(CO)_n]^+$ is observed. The pentamer is the largest cluster that can be observed. Of particular interest is the $[(CO)_2]^+$, that is easily formed and that is the charged equivalent of the well studied van der Waals complex $(CO)_2$ [39,40]. So far spectroscopic data are lacking for the charged dimer, even though matrix data are available that may indicate where to search for vibrational modes [41]. Mixing CO with N_2 yields definitely also mixed clusters $[N_2–CO]^+$ that, however, cannot be directly discriminated because both precursor gasses have a molecular weight of 28 amu. In O_2/N_2 plasma – that is generally hard to run as the O_2 affects the filament – ions $N_2O_2^+$, $[N_3O]^+$ and $[N_5O]^+$ have been found. $[Ar–N_2]^+$ is definitely much easier to produce than $[N_2–O_2]^+$ which reflects the larger difference in IE ($IE(O_2) = 12.07$ eV). Also measurements in pure CO_2 plasma have been performed that mainly show dimer and trimer cluster formation. Again, the actual size distribution will strongly depend on the backing pressure.

The degree of cluster formation is much higher in the expansion than in long and cryogenically cooled discharge cells, such as hollow cathode or magnetically extended negative glow discharges. So far only $[Ar–H_3]^+$ and $[Ar–D_3]^+$ have been spec-

Table 1b
Overview of charge induced complexes formed in supersonic planar plasma using electron impact ionization

400 mbar N_2									
m (amu)	14	28	42	56	84	112	140		
ion	N^+	N_2^+	N_3^+	$(N_2)_2^+$	$(N_2)_3^+$	$(N_2)_4^+$	$(N_2)_5^+$		
intensity	a	s	a	vs	a	w	vw		
120 mbar CO_2									
m (amu)	44	88	132						
ion	CO_2^+	$(CO_2)_2^+$	$(CO_2)_3^+$						
intensity	s	a	w						
400 mbar CO									
m (amu)	28	56	84	112	140				
ion	CO^+	$(CO)_2^+$	$(CO)_3^+$	$(CO)_4^+$	$(CO)_5^+$				
intensity	a	s	w	w	vw				
200 mbar Ar/ 250 mbar N_2									
m (amu)	14	28	42	56	68	80	84	96	
ion	N^+	N_2^+	N_3^+	$(N_2)_2^+$	ArN_2^+	Ar_2^+	N_6^+	$N_2ArN_2^+$	
intensity	a	s	w	s	s	w	w	w	
400 mbar Ar 250 mbar CO									
m (amu)	28	56	68	84	112				
ion	CO^+	$(CO)_2$	$ArCO^+$	$(CO)_3^+$	$(CO)_4^+$				
intensity	a	s	vw	w	vw				
400 mbar N_2/ 5 mbar O_2									
m (amu)	28	30	32	56	58	60	64	86	96
ion	N_2^+	NO^+	O_2^+	N_4^+	N_3O^+	$N_2O_2^+$	O_4^+	N_5O^+	O_6^+
intensity	w	w	s	a	w	w	a	vw	w

The corresponding experimental conditions are listed. vs, very strong; s, strong; a, average; w, weak; vw, very weak.

troscopically identified in a cell discharge [42]. In the expansion seeded molecular species are cooled through binary collisions, while three-body collisions are responsible for the formation of clusters. In the latter process two particles collide and form an activated complex until a third body removes the excess energy and stabilizes the complex via another collision. Low translational temperatures obtained in such supersonic expansions can favour the production of relatively high concentrations of molecular complexes and transient species. Typical densities are roughly in the range of 10^9 to 10^{10} cluster ions/cm^3. As a consequence of the adiabatic cooling of molecular species in a jet expansion their excited internal energy levels are greatly depopulated and the population in the lower rotational and vibrational energy states increases. This effect enhances the state density of the lower energy levels, i.e., decreases spectral congestion, which greatly simplifies recorded spectra.

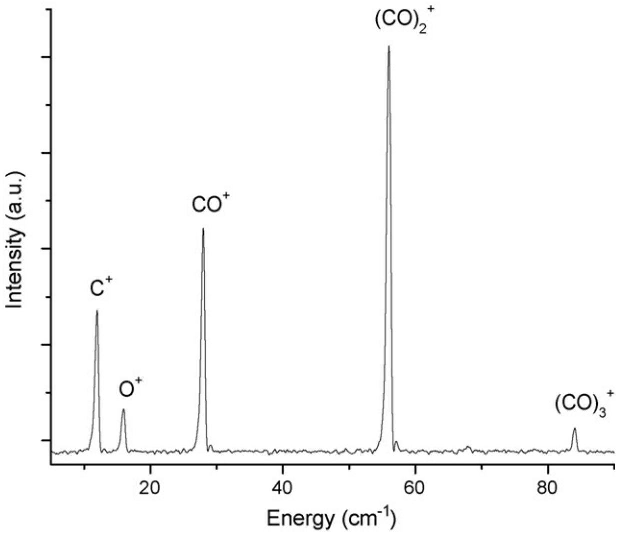

Fig. 5. Mass spectrum of Ar/CO-plasma with partial pressures of 300 mbar of Ar and 100 mbar of CO.

Besides cluster ions also primary ions are formed in abundances of the order of 10^{10} to 10^{12} ions/cm^3, reflecting complexation rates of the order of 10–20%. Many of the smaller species have been studied spectroscopically before, mainly in discharge cells, but it is noticeable that also species such as O_2H^+ and $[O_4H]^+$ are easily formed in an expansion. For more complex molecules discharge cells are generally less suited; spectra are rovibrationally congested, even when applying cryogenical cooling, because of a large number of observable transitions. Therefore, within the context of this work, several more complex species have been studied as well. In a first attempt a number of mixtures with carbon bearing precursors – acetylene, allene, and cyanogens – has been used, among others with the aim to generate long and unsaturated carbon chain radicals of astrophysical interest [43]. Typically species of the form $C_nH_m^+$ are formed with a maximum of about 6 carbon atoms (Table 1c). Also a few cluster ions ($[(C_2N_2)_2H]^+$, $[CO–C_2H_2]^+$ and $Ar–C_2H_4^+$)

Table 1c
Overview of ions and cluster ions formed in carbon bearing plasma using an electron impact planar plasma source

650 mbar 0.3 vol% C_2H_2 in He														
m (amu)	59	62	63	64	65	66	67	74	75	76	77	78	88	100
ion	$C_4H_{11}^+$	$C_5H_2^+$	$C_5H_3^+$	$C_5H_4^+$	$C_5H_5^+$	$C_5H_6^+$	$C_5H_7^+$	$C_6H_2^+$	$C_6H_3^+$	$C_6H_4^+$	$C_6H_5^+$	$C_6H_6^+$	$C_7H_4^+$	$C_8H_7^+$
intensity	w	a	s	vw	vw	vw	vw	s	a	a	a	vw	vw	vw
N_2/ C_3H_3 (700 mbar)														
m (amu)	39	40	56	77	79									
ion	$C_3H_3^+$	$C_3H_4^+$	$(N_2)_2^+$	$C_6H_5^+$	$(C_3H_3)_2H^+$									
intensity	vs	s	s	w	a									
Ar/ C_2H_4 (800 mbar)														
m (amu)	26	27	28	29	39	40	41	53	55	56	57	69		
ion	$C_2H_2^+$	$C_2H_3^+$	$C_2H_4^+$	$C_2H_5^+$	$C_3H_3^+$	$C_3H_4^+/Ar^+$	$C_3H_5^+/ArH^+$	$C_4H_5^+$	$C_4H_7^+$	$C_4H_8^+$	$C_4H_9^+$	$C_6H_9^+$		
intensity	a	s	a	s	a	w	a	w	w	a	s	w		
Ar/ C_2N_2 (700 mbar)														
m (amu)	40	52	104											
ion	Ar^+	$C_2N_2^+$	$(C_2N_2)_2^+$											
intensity	a	s	w											
Ar/ H_2/ C_2N_2 (750 mbar)														
m (amu)	53	105												
ion	$HC_2N_2^+$	$(C_2N_2)_2H^+$												
intensity	s	a												

The corresponding experimental conditions are listed. vs, very strong; s, strong; a, average; w, weak; vw, very weak.

are observed. To form longer carbon chain radicals higher backing pressures will be necessary [6] and this is not possible in a continuous mode, also because the carbon excess in the plasma tends to form short-circuiting layers. In addition, the filament is strongly affected by this type of plasma which shortens the lifetime substantially. In a second attempt, a small heated reservoir has been incorporated in the nozzle system, in order to bring solid volatile species into the gas phase for evaporation temperatures in the range between 70 and 300 °C. Mass spectra have been recorded for argon expansions containing naphthalene, uracil, 1,4 amino-phenol, and catechol. As one may expect, fragmentation occurs but nevertheless, a large abundance of ionized precursor material is routinely obtained, which opens the possibility of systematic infrared spectroscopic studies of larger transients in planar plasma using electron impact ionization. Naphthalene plasma shows a strong mass peak at 128 amu and a ten times smaller mass peak at 102 amu indicating the loss of a $C_2H_2^+$ unit. Cathechol plasma shows a peak at mass 110 with a dominant loss channel at 93 amu (OH loss) and a large number of fragments below 50 amu, which is also found for 1,4 aminopheno. Uracil plasma shows a clear signal at mass 112 amu with loss channels around 69 and 42 amu.

4. Spectroscopic applications

The online monitoring of the plasma by a mass spectrometer is important as this guarantees the presence of a specific ion or cluster ion during a spectroscopic survey. This is essential as theoretical predictions for fundamental modes are hard because of the stronger interaction in the complex. In the case of the Ar–HN_2^+, for example, it has been a long standing problem to assign all vibrational modes as the complexed NH–stretch shifts as much as 700 cm^{-1} compared to the free NH-stretch. This problem was just very recently fully resolved [29,32].

High resolution infrared radiation from a tunable diode laser system is used to search for rovibrational transitions. Details of this setup are available from Ref. [9]. Recent improvements comprise new software for scanning and frequency calibration. Typically a complete diode laser mode (up to 1.5 cm^{-1}) can be recorded with an absolute precision of the order of 0.001 cm^{-1}. An effective detection scheme is obtained by plasma, i.e., concentration modulation by (non)directing the electron beam towards the gas expansion. Plasma modulation as fast as 12 kHz is routinely used by modulating the negative voltage over filament and molybdenum tube. Absorption signals are recorded by phase sensitive detection using lock-in amplifiers. The modulation is directly visible on the mass spectrometric signal and serves as an additional control for good scanning conditions. In addition, this modulation technique has the advantage that it is insensitive to baseline fluctuations (etalons) caused by optical reflections, which is often the limiting factor when applying frequency modulation with diode lasers. The noise of the continuous plasma is low and is further reduced with a band pass filter that is placed in front of an InSb infrared detector. A number of ionic complexes have been studied in this way. One particularly interesting system is the $[N_2–Ar–N_2]^+$ complex that demonstrates that a (partially) charged Ar-atom can act as intermolecular glue. In a recent study the anti-symmetric stretch vibration of this complex has been studied in detail, both experimentally and theoretically [44]. The complex has a linear and centro-symmetric structure that is beautifully reflected in a 5:4 spin-statistical alternation for transitions starting from odd/even *J*-levels. Following several experimental improvements, a new series of high *J*-transitions in the P-branch of $[N_2–Ar–N_2]^+$ has been found and the line positions are listed for the first time here in Table 2. Inclusion of these new transitions in a standard fit for this linear molecule does not change the previously derived constants and the observed–calculated values

Table 2
New rovibrational (high *J*) transitions as observed for the cluster ion $[N_2–Ar–N_2]^+$ upon excitation of the anti-symmetric (NN) stretch

P(*J*)	Observed	Observed–calculated (10^{-4})
35	2286.2578	12
36	2286.1859	18
37	2286.1128	14
38	2286.0417	28
39	2285.9647	−15
40	2285.8920	−14
41	2285.8211	5
42	2285.7445	−32
43	2285.6735	−13
44	2285.6013	−4
45	2285.5260	−26
46	2285.4553	−2
47	2285.3832	10

All values are in [cm^{-1}]. The observed–calculated values are derived from constants as derived in an earlier study [44].

listed in Table 2 are determined for the parameter set as given in [44]. It is important to note that constant plasma conditions are essential in order to assign spectra using spin statistics. Also, for high *J*-values one may expect fine structure splittings due to spin-rotation interaction and an unambiguous assignment of such components becomes only possible when intensities can be compared (see [19]). The new transitions reported here for $[N_2–Ar–N_2]^+$ do not show any splitting or line broadening and the observed FWHM's are limited by the experimental linewidth (mainly residual Doppler broadening) to 100–120 MHz. The direct observation of high *J*-levels seems to contradict the low final rotational temperatures in the jet. As has been observed previously, this effect is partly due to a less efficient cooling for higher rotational levels, increasing rotational temperatures by as much as a factor two to three [5,45].

It is important to note that more processes are induced in the modulated plasma than "only" periodically changing ion densities. Neutral radicals that are formed in the plasma are not visible mass spectrometrically, as the QMS operates in direct observation modus, i.e., without additional ionization and eventual subsequent fragmentation. Production modulation, however, still takes place and neutral radicals are spectroscopically detectable as well. In the expansion also neutral, i.e., van der Waals bonded species are formed that are destroyed in the plasma. An 180° phase shift on the lock-in amplifier output indicates that a signal following destruction modulation is observed. This has been demonstrated for $Ar–H_2O$ in water plasma [46]. There it also was found that even with plasma the final rotational temperature does not exceed 6.5 K for the observed low *J*-transitions. Furthermore molecules, both neutrals and radicals, are state-modulated in the plasma and this is a direct consequence of different vibrational distributions for plasma off (essentially only $v = 0$) and on ($v \geq 0$). In water containing plasma, for example, aimed at observing protonated water dimer, one also will record transitions starting from vibrationally excited states as the modulation scheme does not discriminate between production and state modulation. The latter is quite effective as normally the precursor molecule is involved and it is important to keep the effect in mind to discriminate for example between transitions starting from $[(H_2O)_nH]^+$ and H_2O ($v > 0$). Finally, it has been shown that the rotational temperatures of vibrationally excited species in the plasma expansion are low [14] and this offers potential to extend measurements to higher *v*-values.

In principle, laser spectroscopic investigations are also suited to study the actual molecular processes in the expansion and to test plasma simulations. In the last years a number of studies has been reported that focus on temperature and density distributions as well as chemical processes in (particularly industrial) plasma (see e.g., [47,48]). Also theoretical models that simulate plasma processes in an expanding plasma have been reported in literature [49,50] – mainly for pulsed discharge slit nozzles – and show that unambiguous conclusions are not possible, unless a number of approximations is made. In the present case a theoretical plasma characterization has not been undertaken yet and consequently an efficient use of the source described here is fully dependent on accurate mass spectrometric data.

5. Conclusion

The results of a systematic mass spectrometric survey are presented that demonstrate the performance of an electron impact plasma source and that show the potential of studying cluster ions in direct absorption through supersonic planar plasma, as demonstrated here for new and high *J*-transitions of the $[N_2–Ar–N_2]^+$ complex. Ions and cluster ions with masses up to 250 amu are discussed. Many of the species that are formed in larger amounts have not been studied by spectroscopic techniques so far and an extension towards these systems will definitely further improve the understanding of charged induced interactions at the level of molecular motion.

Acknowledgements

The authors thank J. Bouwman for help during the $[N_2–Ar–N_2]^+$ experiments and Prof. N.M.M. Nibbering for useful discussions. This work is part of the research program of the 'Stichting voor Fundamenteel Onderzoek der Materie (FOM)', which is financially supported by the 'Nederlandse Organisatie voor Wetenschappelijk Onderzoek (NWO)' and of the 'Nederlandse Onderzoeksschool voor Astronomie (NOVA)'. D.V. acknowledges EU support within the integrating infrastructure initiative (RII3-CT-2003-506350–LCVU ACCESS program).

References

[1] E.P.L. Huster, S.G. Lias, J. Chem. Phys. Ref. Data 27 (1998) 413.
[2] S.G. Lias, J.E. Bartmess, J.F. Liebman, J.L. Holmes, R.D. Levin, W.G. Mallard, J. Chem. Phys. Ref. Data 17 (1) (1988) 1.
[3] S.G. Lias, J.F. Liebman, R.D. Levin, J. Chem. Phys. Ref. Data 13 (1984) 695.
[4] G. Hilpert, H. Linnartz, M. Havenith, J.J. ter Meulen, W.L. Meerts, Chem. Phys. Lett. 219 (1994) 384.

[5] D.T. Anderson, S. Davis, T.S. Zwier, D.J. Nesbitt, Chem. Phys. Lett. 258 (1996) 207.
[6] T. Motylewski, H. Linnartz, Rev. Sci. Instrum. 70 (1999) 1305.
[7] R.F. Curl, K.K. Murray, M. Petri, M.L. Richnow, F.K. Tittel, Chem. Phys. Lett. 161 (1989) 98.
[8] T.F. Giesen, A. van Orden, H.J. Hwang, R.s. Fellers, R.A. Provencal, R.J. Saykally, Science 265 (1994) 756.
[9] H. Linnartz, D. Verdes, T. Speck, Rev. Sci. Instrum. 71 (2000) 1811.
[10] T. Haber, A.C. Blair, D.J. Nesbitt, M.D. Schuder, J. Chem. Phys. 124 (2006) 054316, and references therein.
[11] M. Araki, H. Linnartz, P. Cias, A. Denisov, J. Fulara, A. Batalov, I. Shnitko, J.P. Maier, J. Chem. Phys. 118 (2003) 10561.
[12] X.F. Tan, F. Salama, Chem. Phys. Lett. 422 (2006) 518, and references therein.
[13] G. Bazalgette Lacoste-Courreges, J.P. Sprengers, J. Bulthuis, S. Stolte, T. Motylewski, H. Linnartz, Chem. Phys. Lett. 335 (2001) 209.
[14] G. Bazalgette Lacoste-Courreges, J.P. Sprengers, S. Stolte, H. Linnartz, J. Mol. Spectrosc. 205 (2001) 341.
[15] E.J. Bieske, J.P. Maier, Chem. Rev. 93 (1993) 2603.
[16] E.J. Bieske, O. Dopfer, Chem. Rev. 100 (2000) 3963.
[17] J.M. Lisy, J. Chem. Phys. 125 (2006) 132302.
[18] H.-S. Kim, M.T. Bowers, J. Chem. Phys. 93 (1990) 1158.
[19] H. Linnartz, D. Verdes, J.P. Maier, Science 297 (2002) 1166.
[20] H. Verbraak, J.N.P. van Stralen, J. Bouwman, J.S. de Klerk, D. Verdes, H. Linnartz, F.M. Bickelhaupt, J. Chem. Phys. 123 (2005) 144305.
[21] D. Verdes, H. Linnartz, J.P. Maier, P. Botschwina, R. Oswald, P. Rosmus, P.J. Knowles, J. Chem. Phys. 111 (1999) 8400.
[22] E.E. Gerguson, F.C. Fehsenfeld, P.D. Goldan, A.L. Schmeltekopf, Int. J. Mass Spectrom. 32 (1997) 1273.
[23] R.P. Wayne, Chemistry of Atmospheres, Oxford University Press, UK, 1991.
[24] W. Klemperer, Proc. Natl. Acad. Sci. U.S.A. 103 (2006) 12232.
[25] D.A. Wild, E.J. Bieske, Int. Rev. Phys. Chem. 22 (2003) 129.
[26] S.A. Nizkorodov, Y. Spinelli, E.J. Bieske, J.P. Maier, O. Dopfer, Chem. Phys. Lett. 265 (1997) 303.
[27] T. Speck, H. Linnartz, J.P. Maier, J. Chem. Phys. 107 (1997) 8706.
[28] O. Dopfer, R.V. Olkhov, J.P. Maier, J. Phys. Chem. A 103 (1999) 2982.
[29] H. Linnartz, D. Verdes, P.J. Knowles, N.M. Lakin, P. Rosmus, J.P. Maier, J. Chem. Phys. 113 (2000) 2736.
[30] D. Verdes, H. Linnartz, P. Botschwina, Chem. Phys. Lett. 329 (2000) 228.
[31] K. Seki, Y. Sumiyoshi, Y. Endo, J. Chem. Phys. 117 (2002) 9750.
[32] H. Verbraak, M. Snels, P. Botschwina, H. Linnartz, J. Chem. Phys. 124 (2006) 224315.
[33] P. Botschwina, T. Duto, M. Mladenovic, R. Oswald, S. Schmutz, H. Stoll, Faraday Disc. 118 (2001) 433.
[34] J. Dai, Z. Bačić, X. Huang, S. Carter, J.M. Bowman, J. Chem. Phys. 119 (2003) 6571.
[35] K.R. Asmis, N.L. Pivonka, G. Santabrogio, M. Brümmer, C. Kaposta, D.M. Neumark, L. Wöste, Science 299 (2003) 1375.
[36] T.D. Fridgen, T.B. McMahon, L. MacAleese, J. Lemaire, P. Maitre, J. Phys. Chem. A 108 (2004) 9008.
[37] E. Witkowicz, H. Linnartz, C.A. de Lange, W. Ubachs, A. Stoufis, M. Massaouti, M. Velekagris, Int. J. Mass Spectrom. 232 (2004) 25.
[38] A.A. Khan, Chem. Phys. Lett. 319 (2000) 440.
[39] M.D. Brookes, A.R.W. McKellar, Chem. Phys. Lett. 287 (1998) 365.
[40] J. Tank, A.R.W. McKellar, L.A. Surin, D.N. Foruzikov, B.S. Dumesh, G. Winnewisser, J. Mol. Spectrosc. 214 (2002) 87.
[41] W.E. Thompson, M.E. Jacox, J. Chem. Phys. 95 (1991) 735.
[42] S. Bailleux, M. Bogey, H. Bolvin, S. Civiš, M. Cordonnier, A.F. Krupnov, M. Yu Tretyakov, A. Walters, L.H. Coudert, J. Mol. Spectrosc. 190 (1998) 130, and references therein.
[43] T. Motylewski, H. Linnartz, O. Vaizert, J.P. Maier, G.A. Galazutdinov, F.A. Musaev, J. Krelowski, G.A.H. Walker, D.A. Bohlender, Astrophys. J. 531 (2000) 312.
[44] H. Linnartz, D. Verdes, P.J. Knowles, N.M. Lakin, P. Rosmus, J.P. Maier, J. Chem. Phys. 113 (2000) 895.
[45] T. Ruchti, T. Speck, J.P. Connelly, E.J. Bieske, H. Linnartz, J.P. Maier, J. Chem. Phys. 105 (1996) 2591.
[46] D. Verdes, H. Linnartz, Chem. Phys. Lett. 355 (2002) 144.
[47] R. Engeln, K.G.Y. Letourneur, M.G.H. Boogaarts, M.C.M. van de Sanden, D.C. Schram, Chem. Phys. Lett. 310 (1999) 405.
[48] Y. Ionikh, A.V. Meshchanov, J. Röpcke, A. Rousseau, Chem. Phys. 322 (2006) 411.
[49] J. Remy, L. Biennier, F. Salama, Plasma Sources Sci. Technol. 12 (2003) 619.
[50] L. Biennier, A. Benidar, F. Salama, Chem. Phys. 326 (2006) 445.